Research Article

Investigation of the Thermal and Mechanical Properties of Glass Fiber Reinforced ABS/Epoxy Blended Polymer Composite

Ramakrishna Pramod
Mechanical Engineering Department, Amrita School of Engineering, Bengaluru Campus Amrita Vishwa Vidyapeetham, India

Veeresh Kumar Gonal Basavaraja*
Mechanical Engineering Department, National Institute of Technology-Andhra Pradesh, Tadepalligudem, Andhra Pradesh. India

* Corresponding author. E-mail: veereshkumargb@nitandhra.ac.in DOI: 10.14416/j.asep.2024.08.003
Received: 21 May 2024; Revised: 19 June 2024; Accepted: 9 July 2024; Published online: 6 August 2024

Abstract
This research investigates the formation of polymer blends by blending Epoxy LY556 with Acrylonitrile-Butadiene-Styrene (ABS) at weight percentages ranging from 2 to 10% wt. The thermal properties, morphological characteristics, tensile strength, flexural strength, and interlaminar shear strength (ILSS) characteristics of these composites were examined. The X-ray Diffractometer (XRD) and Fourier Transform Infrared Spectrometer (FTIR) studies confirmed the presence of binary blends. The miscibility of epoxy/ABS blends is shown by the presence of a single melting peak in the Differential Scanning Calorimetry (DSC) analysis. The Thermogravimetric Analysis (TGA) findings indicate that epoxy and ABS blends exhibit greater thermal stability than pure epoxy. The tensile strength increased from 183.6 to 380.6 MPa, flexural strength increased from 165.3 MPa to 335.6 MPa, ILSS increased from 32.4 MPa to 72 MPa for 8% wt. of ABS blending, and the laminates witnessed a decrease in density and hardness values. The Scanning Electron Microscopy (SEM) images demonstrate the commendable blending characteristics and the synergistic impact of the ABS/Epoxy composite, yielding superior outcomes to the pure epoxy material.

Keywords: Acrylonitrile-Butadiene-Styrene, Composite material, Epoxy, Fabrication, Interlaminar shear strength, Tensile

1 Introduction

In the meteoric evolution of modern technologies, the synthesis and development of materials with various properties that conventional polymers, metals, and ceramics cannot possess is paramount. Composites have been primarily used for high-performance aerospace, aviation, and sports until recently. However, due to the ever-growing demands for materials with superior properties, composites are now finding relevance in more generic day-to-day applications. A polymer could be strengthened through new fibers, producing a lighter and sturdier material. Materials with a decent number of favorable properties achieved through careful combination with various other substances are primarily in demand. Multiwalled carbon nanotube composites have three percent higher tensile strength and sixty-five percent greater flexural strength [1].

Composite materials are frequently employed in automobile crashworthy structures to sustain axial and non-axial stresses due to their better absorption of energy capability [2], [3]. Polymer matrix composites (PMCs) feature qualities, including a high stiffness-to-weight ratio, a high strength-to-weight ratio, remarkable optical properties, increased fracture toughness, wear, fatigue, thermal expansion, and corrosion resistance properties [4]–[7]. Producing glass fiber composites entails integrating thin synthetic fibers with a tiny diameter into the polymer matrix as the main strengthening component [8]–[10].

Because of their easy production, adaptable configurations and forms, excellent strength, resistance to corrosion, and high strength-to-weight ratio, fiberglass-reinforced plastics (FRP) are used in small surveillance vessels, commercial fishing vessels, and interisland passenger boats and ships [11], [12]. Researchers regularly suggested PMCs such as glass-fiber/Carbon/Arid-reinforced polymers [13]. The Glass Fibre Carbon Reinforced Polymer Composite (GCRC) demonstrates its superiority through increased resistance to indentation. Applications were found in the automotive vehicle body and braking segments and aeroplane radome and brake segments [14]. Glass fiber reinforced plastics (GFRP) is a material that is recommended for usage in the aerospace and automotive industries due to its decreased density, excellent mechanical capabilities, and impressive thermal properties [15]. Compared to other types of glass fibers, E-glass fiber is an important material being researched due to its exceptional qualities. Additionally, e-glass is resistant to heat and corrosion and has a high level of strength. Electrical insulating material industries and vehicle structural sectors are two areas that may benefit from the usage of e-glass [16].

There is a correlation between the stacking arrangement of fabric layers and the performance of tensile and flexural characteristics [17]. Experimental research into the dependence of ply orientation on ultimate tensile strength (UTS), flexural strength, and fatigue strength of woven bidirectional glass fiber-reinforced PMCs revealed that the properties obtain their maximum value for a ply angle of 0 degrees and that the flexural and fatigue properties decrease as the angle increases [18]–[20]. The dependence of the ply orientation and areal density on the tensile characteristics and failure modes of thin-ply carbon fiber reinforced plastic (CFRP) composites was investigated. The results of this study were used to generate a failure diagram that illustrates the many failure modes that occur for varying ply angles and areal densities [21].

Silica nanoparticles improve mechanical characteristics in Bis-GMA/TEGDMA resin blend and composite systems, showing the importance of intermolecular hydrogen bonding [22]. Co-cured compositions of unsaturated polyester (UP) with fire-retardant and char-forming phenolic resins (P.H.) have been studied for their impact on glass fiber-reinforced composite mechanical and fire performance [23]. Utilizing epoxidized waste vegetable oils as a triglyceride source for epoxy resins shows promise, with purified waste oils performing comparably to neat oil at up to 10 wt%. At the same time, higher proportions exhibit a notable plasticizing effect, enhancing mechanical properties in composites [24]. Enhancing conventional epoxy resin through blending with phenolic-urea oligomers as both matrix modifiers and curing agents, followed by characterization of resulting laminates for improved thermal stability, mechanical properties, and chemical resistance [25].

DOPO-reactively flame retarded CE/EP blends improve thermal stability and flammability, with cyanate ester addition compensating for increased glass transition temperature (Tg), enabling high-performance carbon fiber reinforced composites [26]. The adaptability, cheap cost, and customizable features of unsaturated polyester resins (UPRs) are offset by their water susceptibility and fire resistance. Blends, IPNs, composites, and nanocomposites improve UPRs for automotive, construction, and coatings applications while addressing environmental and health issues [27]. Unsaturated polyester resins (UPRs) dominate composites because of their cost-effective chemical resistance. Still, their mechanical qualities need reinforcing for structural functions. Fibers, fillers, and nanoparticles make UPRs suitable for various sustainable engineering applications [28]. Adding phosphorus-containing flame retardants to co-cured unsaturated polyester with phenolic resoles reduces heat release parameters. However, enhanced smoke evolution implies condensed-phase and gas-phase effects. Based on TGA experiments, unsaturated polyester and phenolic resin compatibility improves flame retardant retention in the condensed phase [29]. In bisphenol A cyanate ester (ACE)/ fluorinated poly (aryl ether nitrile) (PFPEN) blends, four bisphenol A glycidyl ether epoxy resins (E06, E12, E20, and E44) improved curing, mechanical, thermal, and adhesive characteristics E20/PFPEN/ACE improved tensile, impact, shear, and peel strength, indicating it might be used in high-performance adhesives and resin matrix composites [30]. Polyethylene glycol (PEG) and epoxy resin are blended in this study, and higher PEG content increases crystallinity and enthalpy but decreases stability and mechanical strength. Higher PEG molecular weight improves stability but weakens mechanical properties [31]–[34]. Glass-fiber bituminous coal tar-epoxy composites show that these composites have higher density and mechanical strength when the coal tar concentration is altered. Additionally, exposure to cryogenic conditions improves their resistance to wear [35].

Materials with excellent tensile and compressive strength, such as ramie fiber composites, exhibit exceptional qualities. The surface flaws in these materials may lead to their fracture and failure at stress levels far below the anticipated value [36]. Weight reduction and greater fuel efficiency were some of the few primary unmet needs of the vehicle industry until the invention of lightweight composite materials. Reducing the weight of a car allows the designer to use a lower amount of power, significantly improving fuel efficiency [37]. G. Chollona *et al*., examined the microstructure and mechanical characteristics of coal tar pitch-based 2D-C/C composites with fillers of carbon blacks and colloidal graphite injected between the U.D. layers of coal tar pitch-based 2D-C/C composites. Including the filler substantially enhanced the flexural strength and interlaminar shear strength [38].

Simon Sembiring *et al*., [39] examined a Bituminous composite that consisted of Amorphous Silica derived from Rice husks. They have determined that the thermal properties of the composite with varied ratios of Silica, the porosity is reasonably reducing, and density and compressive strength rise with the increase in Silica. Addressing impact loading challenges is essential, as optimizing fiber and matrix combinations and leveraging multi-attribute decision-making tools to guide future research in enhancing energy absorption and failure mitigation [40].

ABS's durability, dimensional stability, ease of processing, chemical resistance, and cost-effectiveness make ABS-epoxy resin mixing essential. Adding a thermoplastic phase like ABS improves the fracture toughness of cured unmodified epoxy resins, which are brittle with low fracture toughness. This combination combines the toughness of the thermoplastic modifier with the processing benefits of a thermoset matrix system. Therefore, studying the toughening ability of a bifunctional epoxy resin treated with ABS is essential.

The current investigative work aims to fabricate a polymer matrix mixture of Epoxy blended with acrylonitrile butadiene styrene at varying weight percentages from 2% to 10%. Reinforcement of the acquired polymer matrix with E-Glass fiber through hand layup process. They performed various tests to determine the mechanical properties following ASTM test standards. This study included ABS in the Epoxy network as a toughening agent to get precisely adjusted mechanical characteristics. An extensive analysis was conducted on the phase structures of these mixed polymers, and their relationship with their thermal and mechanical characteristics and qualities was established. The objective was to fundamentally comprehend their mechanical and thermal properties.

2 Materials and Methods

2.1 *Selection of materials and fabrication*

The present study used unidirectional, 200GSM E-glass fibers with a density of 2.54 g/cc, obtained in sheets from Marqtech Ltd, Bengaluru, India. The matrix materials are Araldite LY556, with a density of 1.15 g/cc, and Acrylonitrile-butadiene-styrene (ABS) granules of hardness R110, with a specific density of 1.09 g/cc, which were used for resin blending. The hardener was Aradur HY951, and the resin was obtained from Huntsman India Pvt. Ltd.

2.2 *Preparation of blended resin*

The dissolution process is expedited by using a sonicator equipped with an ultrasonic probe strategically designed to break intermolecular interactions and ensure a homogeneous distribution of components. A frequency of 20 kHz is specifically chosen for its effectiveness in disintegrating the ABS slurry lumps within the resin matrix. Following the initial step of subjecting the mixture of ABS slurry and Araldite LY556 epoxy resin to magnetic stirring, a subsequent phase involves pulsated ultrasonication within the ultrasonicator. This process extends over 45 minutes, employing intermittent pulses lasting 2 seconds each. The controlled application of ultrasonic energy serves to refine the dispersion of ABS within the resin, enhancing the overall blend.

The introduction of the ABS-infused slurry into the resin marks a crucial stage. Subsequently, the composite is subjected to magnetic stirring, ranging from 600 to 1000 rpm. The temperature is carefully maintained at 60 ℃, facilitating the controlled evaporation of highly volatile acetone from the mixture, thus leaving behind a homogeneous blend of ABS in the Araldite LY556 epoxy resin. Stirring persists until a distinctive, uniform swirl motion emerges, typically achieved within 15 to 20 min. This observed motion signifies the attainment of a well-mixed composition, denoting the completion of the intricate process. The meticulous orchestration of these steps ensures the creation of a composite material with a consistent and desirable composition, essential for its intended application.

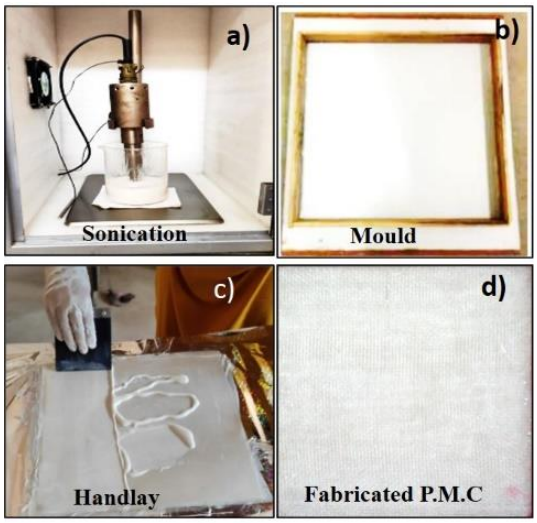

Figure 1: Fabrication process of PMC.

Table 1: Details of the blended resin Composites fabricated.

Sl. No	Composition	Designation
1	E-Glass+100 % Epoxy Resin	Composite 1
2	E-Glass+98 % Epoxy +2% ABS resin	Composite 2
3	E-Glass+96 % Epoxy Resin+4% ABS resin	Composite 3
4	E-Glass+94% Epoxy Resin+6% ABS resin	Composite 4
5	E-Glass+92 % Epoxy Resin+8% ABS resin	Composite 5
6	E-Glass+90%Epoxy Resin+10% ABS resin	Composite 6

2.3 *Fabrication of E-Glass, Epoxy, and ABS resin PMCs*

The composites were meticulously fabricated through a precise manufacturing process to ensure structural integrity and minimal porosity. The hand-lay process involved arranging approximately of accurately cut glass fabric layers, totaling 15. A blended resin-hardener mixture was applied onto the fabric surface, and pressure was applied using hand rollers. Subsequently, the hand layup process was employed, and compression molding took place in a die utilizing a compression molding machine. The mold size was 300 × 300 × 10 mm. The composites fabricated were a 6 mm thickness. This was executed at a pressure range of 8–10 bar and 80–100 °C temperature.

The die remained closed for 24 hours to ensure consistent compaction pressure, which is essential for achieving uniform composite thickness. The applied pressure during compression molding played a crucial role in attaining the desired uniformity in composite thickness. Following the molding process, the plate was carefully removed from the die and subjected to a curing period in an autoclave for an additional 10 hours. The resultant composites exhibited a thickness within the range of 6 mm, as shown in Table 1, and the fabrication process has been shown in Figure 1.

2.4 *Experimental Details*

The test specimens were cut out to the specifications as per ASTM standards. The density of composites in the weight-to-volume ratio was measured according to ASTM D792. The samples were used to research hardness, tensile strength, flexural strength, and inter-laminar shear strength [ILSS]. Scanning electron microscopy (SEM) pictures of composites were acquired by examining them using a JEOL SEM 840 model used for research. Hardness is measured using a Hardness tester from BAREISS, adopting the Shore D scale in accordance with ASTM D2240. A computerized universal testing equipment, the TUE – 400C Fine Spavy Associates type, was used to determine the tensile strength using the ASTM D3039 standard and the flexural strength using the ASTM D790 standard.

The INSTRON 1186 model was used to determine the interlaminar shear strength analysis. When mixed, the TA-DSC 250 Differential Scanning Calorimetry was used to evaluate the curing kinetics of the epoxy resin and ABS resin mixes. Following applying a 40 mL/min-1 nitrogen flow rate, the samples were heated at ten °C/min from 10 to 400 degrees Celsius.

The TA-DSC 250 differential scanning calorimetry (DSC) device was used to evaluate the glass transition temperatures (Tg) of the ABS/Epoxy blends. A temperature range of 20 to 250 degrees Celsius was used for the experiments, and a heating rate of 10 degrees Celsius per minute was used. Additionally, a nitrogen flow rate of 50 milliliters per minute was used. The thermogravimetric analyzer (TGA/DSC2) was used to evaluate the ABS/epoxy composite's thermal stability performance. The specimens were subjected to thermal examination in a nitrogen atmosphere, with the temperature being raised from room temperature to 700 degrees Celsius at a rate of 20 degrees Celsius per minute. The specimen is subjected to an oscillating force in the DMA process, and the material's response to this force is considered. On the other hand, the modulus

acquired from DMA measurements does not perfectly correlate with Young's modulus, which is determined using the standard stress-strain curve.

A GABO Qualimeter dynamic mechanical analyzer was used to determine the dynamic mechanical characteristics. The multi-frequency-strain mode was used to ascertain the storage modulus (E'), the damping factor (tanδ), and the glass transition temperatures (Tg). Research was carried out using a three-point bending (TPB) technique at a frequency of one hundred hertz. The samples were heated at three kelvins per minute from the original ambient temperature to 380 degrees Kelvin to conduct the tests.

3 Results and Discussions

3.1 *Microstructure and FTIR studies of the Fabricated E-Glass, Epoxy, and ABS resin PMCs*

The microstructures of the fabricated E-Glass, Epoxy, and ABS resin PMCs are depicted in Figure 2. These images vividly illustrate the seamless integration and homogeneous bonding between the constituents: E-glass fibers, Epoxy matrix, and ABS resin. This homogeneous bonding is pivotal as it significantly amplifies various physical characteristics and mechanical properties, including hardness, tensile strength, and flexural strength.

These PMCs foster effective load transfer mechanisms from the continuous matrix to the reinforcing materials by fostering homogeneous bonding. Consequently, this synergy fortifies the composite's resistance against crack initiation and subsequent propagation, thereby endowing it with a heightened load-carrying capability. The effective integration achieved through homogeneous bonding lays the foundation for superior performance and durability in structural applications.

The pristine ABS showed all the characteristic bands at 3150–2900 cm^{-1} (C-H stretching of CH, CH_2, and phenyl ring), 2238 cm^{-1} (-CN stretching in acrylonitrile), 1633 cm^{-1} (-C=C stretching in butadiene), 1550–1450 cm^{-1} (-C-H bending in phenyl ring of styrene), and 850–700 cm^{-1} (trans-1-4 C=C stretching, bending of = C-H in phenyl). The I.R. spectrum of pristine EVA showed the characteristic bands at 3100–2850 cm^{-1} (C-H stretching of CH_2 and CH_3), 1755 cm^{-1} (C=O stretching), 1,391 cm^{-1} (C-H bending), 1275 and 1030 cm^{-1} (C-OCO and O-CO stretching), and 750 cm^{-1} (C-H rocking). Epoxy resins acquire exceptional characteristics due to their complete crosslinked structures. The spectra of the pure epoxy resin exhibited the usual absorption bands, with a distinct absorption band representing the OH bond seen between 3650 and 3250 cm^{-1} [39]. However, the observed peak is brief because of the limited quantity of hydroxyl (OH) groups in the molecule of this resin. The band at 918 cm^{-1} (within the range of 960 to 850 cm^{-1}) signifies the presence of the epoxy group. At the same time, the peak at 1100 cm^{-1} shows the existence of an aromatic ether group. The reduction in the peaks around the OH bond represents the blending of the ABS and Epoxy resin. It is evident from the FTIR results shown in Figure 3.

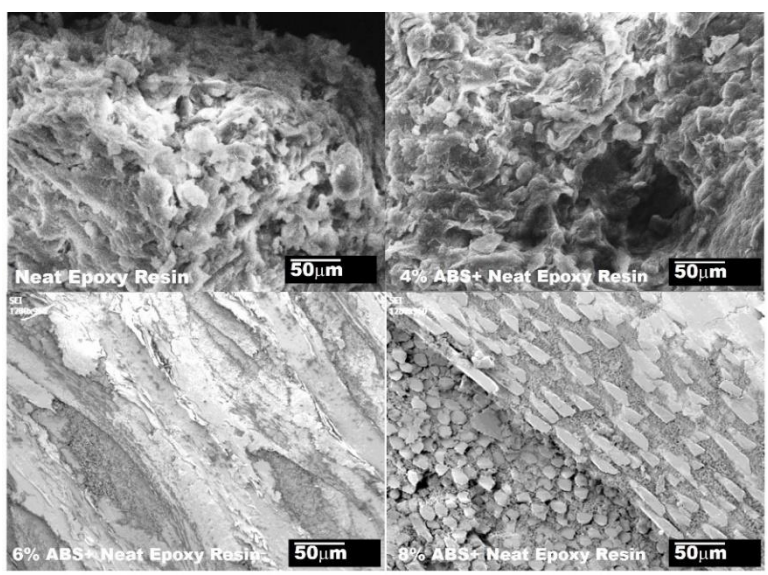

Figure 2: SEM images of the E-Glass, Epoxy, and ABS resin PMCs.

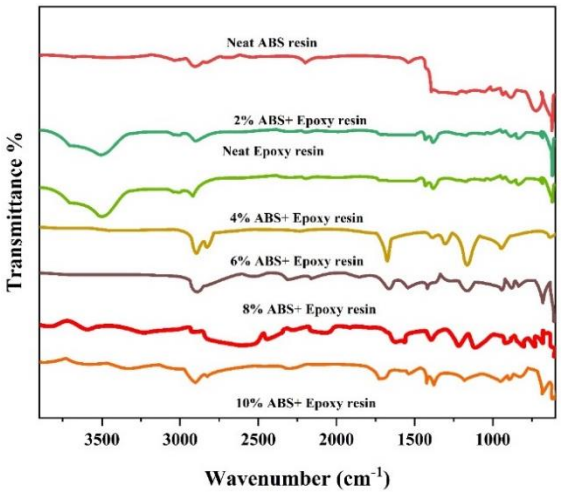

Figure 3: Spectra of neat ABS/Epoxy and combination of blends of ABS/Epoxy.

The blending has been effective, and a compatibilizer has been used. Maleic anhydride (M.A.) is recognized for its potential as a functional monomer capable of enhancing thermoplastic surface polarity and miscibility. In the context of our current investigation, M.A. serves as an effective compatibilizer, facilitating the blending of resins. Due to its propensity to form partially miscible blends with a wide array of thermoplastics and elastomers, ABS has garnered significant commercial traction, particularly within the automotive and electronic industries. The observed reduction in peak intensity around the C=C stretching vibrations (at 1,605 cm^{-1}) [40] can be attributed to the compatibilizer effect within the resin system. This phenomenon underscores the positive influence of M.A. as a compatibilizer, facilitating improved compatibility and interaction between the constituent resins. As a result, the resin system exhibits enhanced homogeneity and potentially improved mechanical and surface properties, rendering it well-suited for various industrial applications.

3.2 *Density and hardness of E-Glass, Epoxy, and ABS resin PMCs*

The density of Acrylonitrile Butadiene Styrene (ABS) is notably lower than that of both Epoxy and the reinforcing material. This characteristic becomes particularly significant as the ABS component proportionately increases within the polymer composites, decreasing the overall density of the PMC. Figure 4 illustrates this trend, showcasing a gradual reduction in density as the content of ABS rises in the laminate. Five trials were taken, and each trial's density values were averaged. Figure 4 shows that as the ABS content increases from 2 to 10%, there is a 4.54% decrease in the density of the composites. This successful manipulation of composite materials results in a lower percentage of porosity.

Further, the adoption of ABS is to manufacture lighter composites with better mechanical and thermal characteristics. Significantly, this decline in material density does not impact the hardness of the fabricated composites. The hardness of the composite material is intricately tied to its composition, microstructure, and inherent features, with the reduction in density being offset by other reinforcing factors. As depicted in Figure 4, the composites are effectively fabricated, and most exhibit porosity levels within 5%. This indicates the success of the fabrication method and curing process, signifying effective blending and thorough curing of the resin components. The careful control of porosity levels underscores the precision and reliability of the manufacturing process, ensuring the integrity and quality of the resulting composite materials [41].

The ASTM D2240 Type D scale was employed as the standard for the hardness test, utilizing a Shore Durometer equipped with a hardened steel rod featuring a 1.3 mm diameter, 30° cone, and 0.79 mm diameter. As is common in various hardness tests, the Durometer gauges the depth of an indentation in the material generated by a specified force applied through a standardized presser foot. Five trials were taken, and each trial's hardness values were average. This indentation depth is influenced by factors such as the material's hardness, its viscoelastic properties, the configuration of the presser foot, and the duration of the test.

In Figure 5, a discernible trend emerges as the ABS content increases within the PMC – the hardness experiences a consistent decline to 57.14% as the ABS content increases from 2 to 10% composites. This phenomenon can be attributed to the inherent softness of ABS, characterized by a Shore D hardness ranging between 55–60. ABS is notably softer than the Araldite LY556 epoxy and the E-glass fiber. Consequently, with an augmented concentration of ABS in the composite, the overall hardness of the ABS, Araldite LY556 epoxy, and the E-glass PMC undergoes a proportional decrease [42].

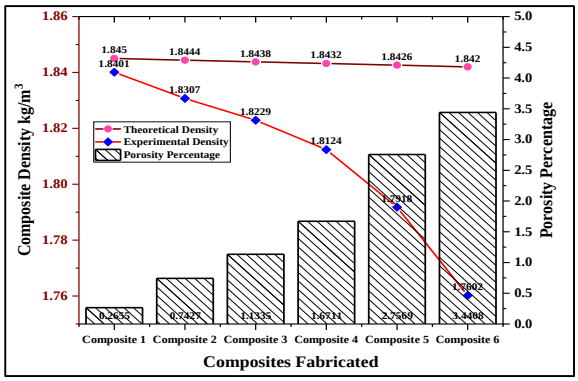

Figure 4: Variation of Density and porosity percentage in the E-Glass, Epoxy, and ABS resin PMCs Fabricated.

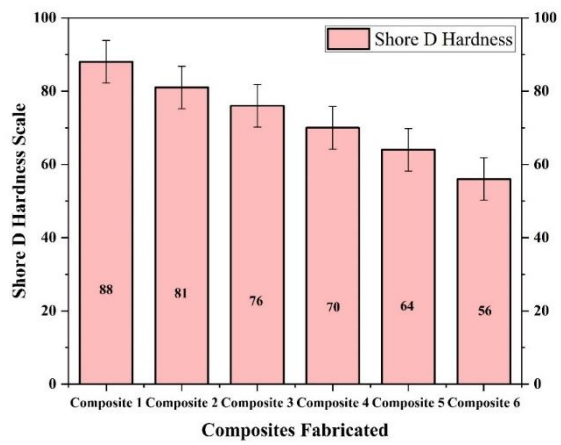

Figure 5: Variation of Shore Hardness in the E-Glass, Epoxy, and ABS resin PMCs.

3.3 *Thermal properties of E-Glass, Epoxy, and ABS resin PMCs*

The DMA analysis in this study encompassed the determination of the storage modulus and the damping factor (tan δ), providing valuable insights into the dynamic properties of the six composites under investigation. The storage modulus, a measure of a material's tendency to exhibit elastic characteristics in a solid state, reflects the viscoelastic properties induced by molecular-level movement when subjected to external stress. The damping factor, represented by tan δ, characterizes the transition from brittle to rubbery states in response to temperature changes. Across all temperatures, the storage modulus was found to have significantly increased for higher resin percentages due to the research into the impact of fiber content on dynamic characteristics. This reinforcing effect was especially prominent above the glass transition temperature of the matrix. This may be due to the significant disparity in mechanical characteristics between the matrix and the resin when the material changes from a state of glass to a rubbery one [43].

The macromolecular chains undergo restructuring and alignment under dynamic tension, reaching their maximum length before breaking in ideal circumstances. However, entrapments and spreading of polymer chains in composite materials limit this scenario. The continuous decrease in the degree of crystallinity of Epoxy and ABS contributes to increased strength in polymeric materials. At elevated temperatures, such as 100 °C, the melting enthalpy of Epoxy absorbs heat in the polymeric material, leading to deformation. Composites often necessitate a Maleic Anhydride compatibilizer agent to mitigate interfacial tension between the matrix and fibers, enhancing mechanical properties. The arrangement of threads and voids within the composite significantly influences energy dissipation during deformation cycles, impacting tan δ values and, consequently, the reinforcement effect [44].

The ABS-Epoxy blend exhibited superior results up to 120 °C, indicating crystal structure formation at regular intervals. The tan δ peak for both ABS and Epoxy showcased a layer-absorbing effect responsible for the dynamic properties of individual polymers without any combinations. Figures 6 and 7 portray the storage modulus and the impact of the damping factor for fabricated pristine ABS/Epoxy and composites [45].

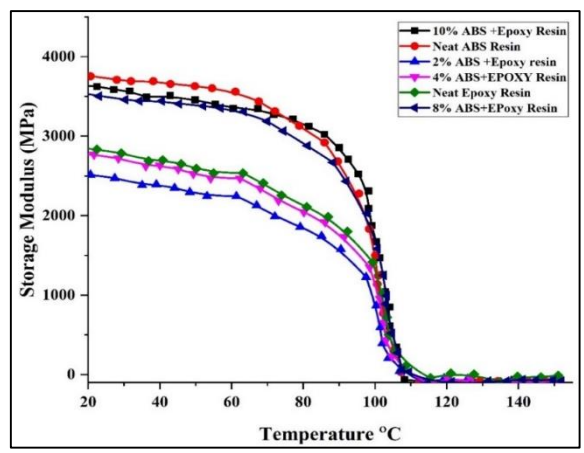

Figure 6: The Storage modulus of the blended resin system and neat Epoxy/ABS resin.

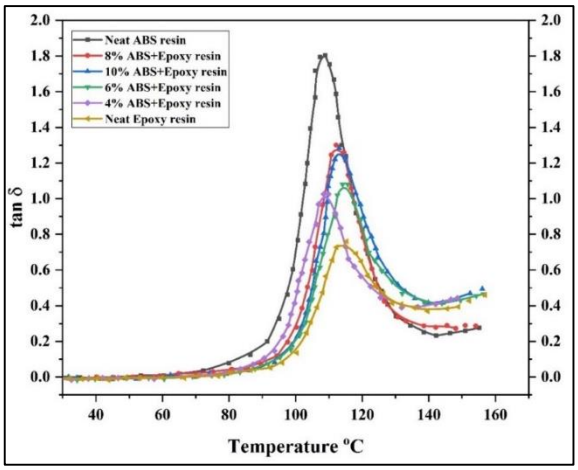

Figure 7: The damping factor of the blended resin system and neat Epoxy/ABS resin.

The glass state exhibited a noteworthy elevation in the storage modulus compared to its relatively low and stable nature in the rubber state. The glass transition zone showed a substantial decrease, marking the transition from a higher initial value in the glass state to a lower value characteristic of the rubber state. Compared to neat Epoxy resin, the composites displayed elevated storage modulus (E0) values, indicating increased stiffness resulting from the physical interaction between fibers and the polymeric matrix (ABS/Epoxy). In studies involving polymer/fiber, the storage modulus, integral to the mechanical perspective, correlates consistently with the tensile modulus, both being substantially affected by material stiffness. The analysis revealed a slight increase in the storage modulus with temperatures up to approximately 78 °C, potentially attributed to an enhanced reinforcement effect arising from tightly bonded E-glass fibers interacting with the surrounding ABS/Epoxy matrix at elevated temperatures [46].

Figure 7 shows the damping factor values maintaining a consistently diminutive scale, exhibiting minimal fluctuations between the glassy and rubber states. Notably, the values observed in the glassy state surpass those in the rubber state, highlighting a distinctive difference. Notably, the loss modulus attains its peak within the glass transition zone, signifying a pivotal range where the material experiences the most significant energy dissipation. This observation sheds light on the dynamic interplay of material properties during the transition from the glass to the rubber state, emphasizing the nuanced behavior of the storage and loss moduli in response to varying states and conditions [47]. The addition of E-Glass fibers contributes to the reinforcement effect above the maximum damping factor (tan δ) in the elastic plateau, as evidenced by the observed trends in storage modulus. This dynamic mechanical behavior is consistently observed across all fibers employed in this study. It emphasizes the intricate interplay between fiber content, matrix properties, and temperature in shaping composite materials' dynamic response and mechanical performance. After the epoxy resin has fully cured, it forms a rigid and fragile structure due to its densely interconnected three-dimensional network. The brittleness of epoxy resin results in a low fracture toughness, which restricts its potential uses and requires the addition of high-toughness properties. Over the last several decades, there has been a significant focus on researching methods to strengthen epoxy resin. Different modifiers, such as hard additives and flexible polymers, have effectively mitigated the intrinsic brittleness of epoxy resin [48].

This study integrated Acrylonitrile Butadiene Styrene (ABS) into the Epoxy network to enhance mechanical properties, providing meticulous exploration of the phase structures in these blended polymers. The correlation between these structures and their thermal and mechanical behaviors was investigated to gain a fundamental understanding of their properties.

The Heat Deflection Temperature (HDT) of neat ABS resin stands at approximately 83 °C. In comparison, the Epoxy/ABS/E-Glass fiber composites demonstrate significantly elevated HDT values of 114 °C. This marks a substantial improvement, with all composites displaying HDT values 10–20 °C higher than those of neat Epoxy and ABS resin. The positive correlation between HDT and E-Glass fiber content underscores the increased load-transferring ability within the composite under test conditions.

Figure 7 shows the damping factor values maintaining a consistently diminutive scale, exhibiting minimal fluctuations between the glassy and rubber states. Notably, the values observed in the glassy state surpass those in the rubber state, highlighting a distinctive difference. Notably, the loss modulus attains its peak within the glass transition zone, signifying a pivotal range where the material experiences the most significant energy dissipation. This observation sheds light on the dynamic interplay of material properties during the transition from the glass to the rubber state, emphasizing the nuanced behavior of the storage and loss moduli in response to varying states and conditions [49]. The addition of

E-Glass fibers contributes to the reinforcement effect above the maximum damping factor (tan δ) in the elastic plateau, as evidenced by the observed trends in storage modulus. This dynamic mechanical behavior is consistently observed across all fibers employed in this study. It emphasizes the intricate interplay between fiber content, matrix properties, and temperature in shaping composite materials' dynamic response and mechanical performance. After the epoxy resin has fully cured, it forms a rigid and fragile structure due to its densely interconnected three-dimensional network. The brittleness of epoxy resin results in a low fracture toughness, which restricts its potential uses and requires the addition of high-toughness properties. Over the last several decades, there has been a significant focus on researching methods to strengthen epoxy resin. Different modifiers, such as hard additives and flexible polymers, have effectively mitigated the intrinsic brittleness of epoxy resin [50].

This study integrated Acrylonitrile Butadiene Styrene (ABS) into the Epoxy network to enhance mechanical properties, providing meticulous exploration of the phase structures in these blended polymers. The correlation between these structures and their thermal and mechanical behaviors was investigated to gain a fundamental understanding of their properties.

The Heat Deflection Temperature (HDT) of neat ABS resin stands at approximately 83 °C. In comparison, the Epoxy/ABS/E-Glass fiber composites demonstrate significantly elevated HDT values of 114 °C. This marks a substantial improvement, with all composites displaying HDT values 10–20 °C higher than those of neat Epoxy and ABS resin. The positive correlation between HDT and E-Glass fiber content underscores the increased load-transferring ability within the composite under test conditions.

The storage modulus, a key indicator of stiffness variation with temperature, exhibits heightened sensitivity to changes in molecular mobility, especially in the proximity of the glass transition region. As temperature increases, molecular chain stiffness undergoes significant alteration, directly impacting the storage modulus. Generally, the modulus decreases with rising temperature, particularly above the glass transition temperature, attributed to increased molecular motion [51].

Above the glass transition temperature, a rapid decrease in modulus is observed across all samples. The tangent delta (tan δ), intricately linked to a material's damping characteristic, is crucial. A higher tan δ value signifies superior damping and energy dissipating capabilities, primarily due to reduced reinforcing effects in a fiber-reinforced polymer matrix composite. Notably, the peak temperature of tan δ (around 118 °C) for the 8% ABS+Epoxy composite experiences a significant shift to higher temperatures by approximately 7°C. The introduction of E-Glass fibers into ABS/Epoxy resin restricts molecular mobility, reducing the loss modulus and decreasing tan δ. This underscores the influence of fiber reinforcement on the dynamic mechanical properties of the composite material [52].

The thermal analysis results in Figure 8 provide valuable insights into the degradation characteristics of the pristine epoxy polymer and its composite formulations, further enhancing our understanding of the material's behavior under varying conditions. Notably, the degradation process unfolds in three distinct phases, with the initial two phases playing a pivotal role in generating a resilient carbonaceous residue, particularly at lower temperatures. The third phase is intricately linked to oxidizing the remaining carbonaceous char [53].

The employment of Thermogravimetric Analysis (TGA) emerges as a potent approach for unraveling the intricate processes involved in polymer breakdown, encompassing both physical and chemical alterations. A noteworthy discovery is an observed correlation between the heating rate and the onset of degradation. Higher heating rates prompt a shift towards elevated temperatures, attributed to the reduced residence time that impedes the efficient transfer of heat to the reactants' core, consequently delaying the thermal degradation process [54].

An intriguing observation lies in the presence of events associated with pure Acrylonitrile Butadiene Styrene (ABS) degradation in assessing the fabricated composites. However, these occurrences exhibit diminished magnitudes directly proportional to the composite's composition. ABS degradation unfolds in two distinct stages, with the initial stage spanning 300 to 470 °C and the subsequent phase between 470 and 600 °C, involving a substantial weight decrease. This weight loss is primarily attributed to the vulnerability of regions rich in butadiene and styrene to degradation. Further examination of the thermal analysis data reveals a positive impact of ABS introduction on the thermal stability of epoxy-based composites. The temperature at 50% mass loss (T50%) for the base epoxy is around 395 °C, while for ABS resin, it is approximately 460 °C. With the addition of ABS to the neat epoxy polymer, T50% increases by 30–40 °C, indicating enhanced thermal stability.

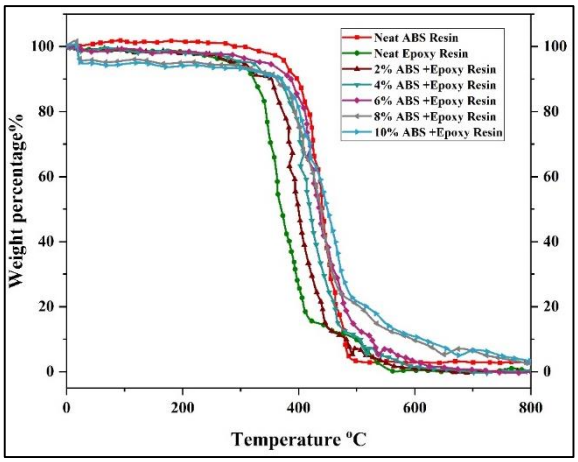

Figure 8: Variation of TGA Curves for Epoxy/ABS blended resin composites.

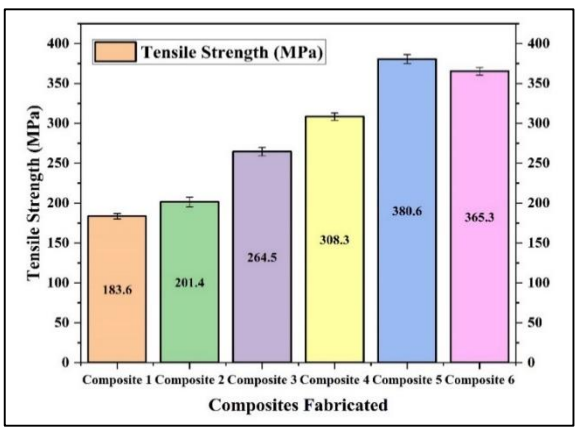

Figure 9: Variation of Tensile Strength in the E-Glass, Epoxy, and ABS resin PMCs.

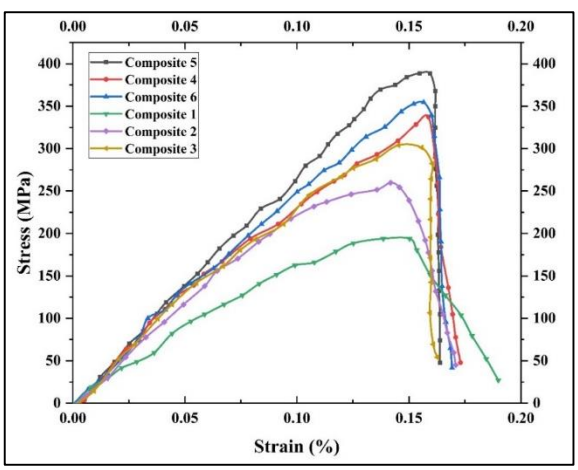

Figure 10: Variation of Tensile Stress and Strain in the E-Glass, Epoxy, and ABS resin PMCs.

The residue at 600 °C for the base Epoxy/ABS composite is 2.4%, in contrast to the complete decomposition of the neat epoxy polymer at the same temperature. This comprehensive understanding clarifies the thermal properties of epoxy composites and facilitates the optimization of their performance attributes [55].

3.4 *Mechanical properties of E-Glass, Epoxy, and ABS resin PMCs*

Nevertheless, the limited bonding and compatibility between fillers and the matrix sometimes impede substantial improvements in toughness in stiff additive-toughened systems. On the other hand, polymer blending is a novel and efficient approach to enhancing the desired characteristics of cured epoxy resin by merging the advantageous qualities of two or more polymers. Several important elements determine how efficient flexible components are in reinforcing the matrix. These factors include the size and configuration of the dispersed phase, the degree of crosslinking within the matrix, and the stickiness at the interface between the components [56]. When it comes to the overall performance of the thermosets produced by a two-phase epoxy system, the size of the second-phase domains is the primary factor determining everything. During fracture growth and deformation, the size should be suitably matched to activate a number of toughening processes. These mechanisms include cavitation, particle bonding, crazing, crack deflection, and shear yielding. It is important to note that the various characteristics of the procedures employed to enhance epoxy resins are highlighted by the intricate interaction between modifiers and matrix properties [57].

3.4.1 The tensile strength of E-Glass, Epoxy, and ABS resin PMCs

The tensile strength test was conducted as per the ASTMD3039/3039M-08, a thin flat strip of material having a constant rectangular cross-section mounted in the grips of a mechanical testing machine and loaded in tension while recording load. The maximum load carried before failure determines the material's ultimate strength. The fibers and resin undergo elastic deformation at low loading levels, and the bending and displacement modes exhibit a linear relationship. Three trials were conducted for each composite, and the average values were considered. This implies that if the load applied to the sample is removed, it will

revert to its original shape. The resin matrix exhibits a yield phenomenon when subjected to higher loadings. When the load exceeds the breaking strength of the resin, the cracks in the matrix enlarge and generate other cracks. However, the incorporation of blended resin systems prevents the development of these additional fractures due to the reinforcement of the matrix system [58].

Consequently, the load-displacement curve exhibits nonlinearity, resulting in a reduction in stiffness. Due to the continuous expansion of fractures and the formation of new cracks, some sections of the load-displacement curve see considerable decreases. The fibers in the reinforcing section of the sample experience fracture as the sample's deformation rises, reducing the sample's load-bearing capacity until the fibers irrevocably break. Figures 9 and 10 (Stress and Strain diagram) show that as the content of ABS increases, the tensile strength increases from 183.6 MPa to 380.6 MPa, with a maximum increase of 103.34%. Still, the tensile strength decreases upon further increase in the content of ABS, i.e., From 8% to 10%. This is due to increased void in the matrix upon increased impurity (ABS) addition. As the content of ABS is increased to 10%, the increased void in the matrix leads to a decrease in tensile strength. ABS resins enhance the tensile strength of the composites, as demonstrated through the DMA parameters.

3.4.2 The flexural strength of E-Glass, Epoxy, and ABS resin PMCs

Flexural strength testing was done with standard *ASTMD790* test methods for flexural properties of unreinforced and reinforced plastics and electrical insulating materials. Three trials were conducted for each composite, and the average values were considered. A three-point bending mechanism is used to calculate the flexural strength of the specimen. Figures 11 and 12 (Flexural Stress and Strain diagram) show that as the content of ABS increases, the flexural strength increases from 165.3 MPa to 335.6 Mpa, and a maximum increase of 103.56% was witnessed.

The flexural test is a valuable indicator for assessing the material's brittleness, with brittle materials typically exhibiting abrupt and unpredictable fractures. In contrast, ductile materials show signs of deformation before reaching the fracture point. In the context of bending stress, the strength of fibers on the sides plays a crucial role in resisting fracture. In our investigation, the breaking load of blended resin glass composites surpasses that of pure Epoxy/E-Glass composites. Notably, the breaking load of blended resin E-glass composite demonstrates a twofold increase compared to polyester E-glass composite. This heightened breaking load underscores the superior mechanical strength and resistance to fracture in the blended resin E-glass composite.

Moreover, the elongation percentage of the blended resin E-glass composite surpasses that of neat epoxy composites, indicating more excellent ductility. This enhanced ductility is a favorable characteristic, suggesting improved deformability and resilience in response to stress. In summary, the results from the tensile test highlight the superior performance of the blended resin E-glass composite compared to other neat epoxy composites. The combination of blended resin with E-glass reinforcement enhances breaking load. It promotes increased ductility, making it a promising candidate for applications where superior mechanical properties are essential [59].

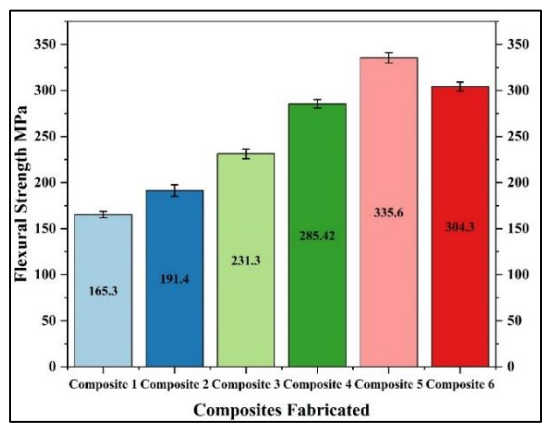

Figure 11: Variation of Flexural Strength in the E-Glass, Epoxy, and ABS resin PMCs.

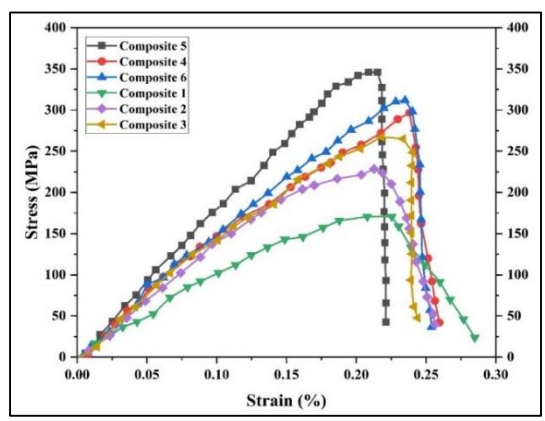

Figure 12: Variation of Flexural Stress and Strain in the ABS/Epoxy resin PMCs.

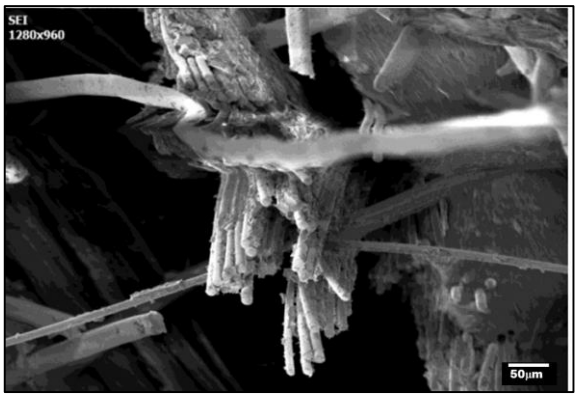

Figure 13: Fractured SEM surfaces of ABS/Epoxy resin PMCs after the tensile strength test.

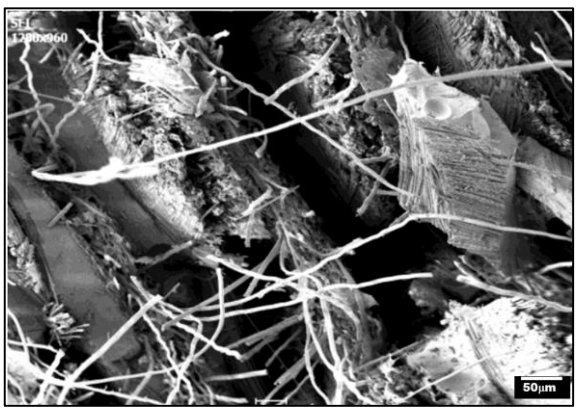

Figure 14: Fractured SEM surfaces of ABS/Epoxy resin PMCs after flexural strength test.

Within the context of crack propagation in a resin system under tensile and flexural testing, as shown in Figures 13 and 14 consisting of Epoxy and ABS, it is well-recognized that forming voids within the flexible phase is essential for maintaining a strong bond between the two materials. During expansion, stress is localized in the submicron domains of the material and the areas around them. The difference in Poisson ratio and Young's modulus between the resin matrix and the E-Glass fiber phase causes the concentration.

This stress concentration results in the enlargement and distortion of voids in the direction perpendicular to the crack's growth path. As the specimen stretches, the empty spaces enlarge and penetrate the mixed resin structure, experiencing plastic deformation. Ultimately, they combine to form small empty spaces called microvoids, which develop into fractures. The stability of these cavities, formed inside the composite due to a flexible phase in a brittle matrix, is significantly influenced by the degree of interfacial adhesion. The cavities in this system remain stable due to the prevailing solid interfacial adhesion. The energy needed to spread these hollow spaces is significantly augmented, efficiently using external energy and hence boosting the overall durability of the material. Significantly, it is considered that the presence of cavities impacts the stress distribution in the surrounding area and enables localized deformation of the network. This serves as a method to absorb excessive energy by promoting shear yielding. The complex interaction between voids and interfacial adhesion enhances the material's stability, general resilience, and capacity to absorb energy [60].

3.4.3 The impact strength and ILSS of E-Glass, Epoxy, and ABS resin PMCs

The Impact Strength test, conducted by ASTM D256, employed an Izod impact tester to determine plastics' Izod pendulum impact resistance. Specimens, prepared per ASTM D256 specifications (10×10×55 mm), featured a 45° V-notch with a 2 mm depth and a 0.25 mm root radius. The impact testing machine's pendulum, set at a specific height, was released onto the specimen's opposite end of the notch, resulting in a fractured sample. The absorbed energy required for two fresh fracture surfaces was recorded, with impact toughness influenced by matrix and interface behavior, encompassing fiber debonding, fiber pull-out, and fiber deformation. Three trials were conducted for each composite, and these values' averages have been considered.

ABS resin, exhibiting a higher energy dissipation capability than E-glass fibers, was pivotal in enhancing impact strength. The blended ABS/Epoxy resin structure demonstrated effective energy damping and absorption under impact loads, facilitating the transfer of impact stresses. Additional energy dissipation processes, such as fiber pull-out, fiber-matrix debonding, and the inhibition of fracture propagation, contributed to the overall toughening effect and an increase of a maximum of 90.07% was observed.

Integrating these energy dissipation processes resulted in a prolonged crack deflection path, enhancing trans-laminar fracture toughness and overall impact energy absorption. Critical factors like stress distribution and maximum elongation significantly contributed to the observed improvement in impact behavior [61].

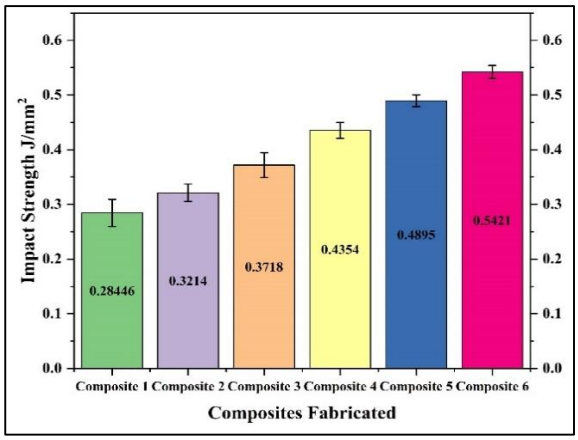

Figure 15: Variation of Impact Strength in the E-Glass, Epoxy, and ABS resin PMCs.

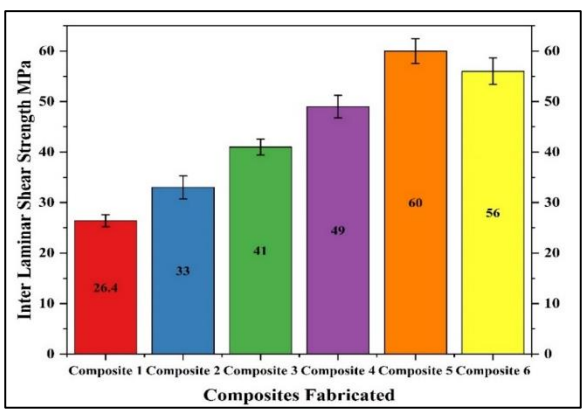

Figure 16: Variation of ILSS in the E-Glass, Epoxy, and ABS resin PMCs.

In summary, the impact strength of the samples displayed an increase with higher toughness strength, underscoring the crucial role of ABS resin in enhancing the impact behavior of the blended resin composites, as shown in Figure 15. This observation emphasizes the importance of material composition and toughening mechanisms in determining the impact performance of composite materials. The study on the impact of ABS resin on the interlaminar shear properties of blended resin composites at normal temperatures produced valuable insights, as shown in Figure 15. The Interlaminar Shear Strength (ILSS) parameter showed a significant pattern, rising as the percentage of ABS resin increased to 8 wt.% and then declining, as shown in Figure 16. This result suggests that increasing the amount of ABS resin in the epoxy resin blend favored the ILSS properties. It improved the ability of the material to absorb energy and reduced the creation of voids in the composite laminate [62], [63].

The observed enhancement in ILSS indicates that adding ABS resin, specifically up to 8%, to the original epoxy matrix increased its capacity to transmit and distribute stress efficiently. The improvement may be ascribed to the homogenous blending technique, in which the high shear modulus of ABS [230 MPa] played a role in strengthening the epoxy matrix by 127.72%. Consequently, the stress transfer improved, allowing the composite samples to endure a higher load. Consequently, including ABS resin in the epoxy-based composites increased the composite specimens' ILSS. This demonstrates the beneficial effect of adding ABS resin on the structural stability and ability to bear composite loads [64], [65].

4 Conclusions

The investigation into PMC has brought forth noteworthy findings, particularly concerning the influence of ABS reinforcement material on various properties. A discernible trend emerges, indicating a reduction in density and hardness as the weight percentage of ABS increases, making the composite lighter than traditional laminates. Microscopic examination of the newly blended resin composites reveals uniform resin blending and acceptable porosity levels after curing, even with an increase in ABS resin from 2% to 10%. The TGA thermal analysis highlights an improvement in the thermal stability of the composites with the inclusion of ABS resin. The shift in peak degradation temperature towards higher values indicates a significant impact on the thermal stability of the blended resin composites. Adding ABS resin enhances the storage modulus, indicating increased stiffness due to uniform resin blending. This hinders chain mobility, making it challenging for polymer chains to move. As the percentage of ABS resin increases, the storage modulus decreases. The damping factor sees a noticeable rise, signifying improved energy absorption capabilities in the composites. Mechanical properties such as tensile and flexural strengths exhibit a substantial increase from 2% to 8% of ABS weight percentage, showcasing improved values with polymer reinforcement. This enhancement bodes well for the laminates, suggesting an overall strengthening effect. However, beyond 8%, a decrease in properties is observed, attributed to voids developing due to increased impurity addition in the matrix. The impact strength of the PMC experiences a notable rise from

0.285 J/mm² to 0.542 J/mm², accompanied by a substantial increase in ILSS from 32.4 MPa to 72 MPa. These improvements are linked to the increased percentage of ABS, enhancing the matrix's energy absorption capabilities and stress distribution. The observed enhancements in mechanical and thermal properties suggest that the utilization of the composite, as opposed to the base material, holds the potential for superior outcomes. These findings contribute valuable insights into optimizing PMC for diverse applications, showcasing the significance of tailored resin blending for improved material performance.

Acknowledgements

We sincerely thank the management of Amrita Vishwa Vidyapeetham, Bengaluru Campus and NIT, Andhra Pradesh, for extending all support for the work.

Author Contributions

R.P.: conceptualization, investigation, reviewing and editing; R.P.: investigation, methodology, writing an original draft; V.K.G.B.: research design, data analysis; V.K.G.B.: conceptualization, data curation, writing—reviewing and editing, funding acquisition, project administration. All authors have read and agreed to the published version of the manuscript.

Conflicts of Interest

The authors declare no conflict of interest.

References

[1] O. Demircan, A. Al-darkazali, İ. İnanç, and V. Eskizeybek, "Investigation of the effect of CNTs on the mechanical properties of LPET/glass fiber thermoplastic composites," *Journal of Thermoplastic Composite Materials*, vol. 33, no. 12, pp. 1652–1673, 2020, doi: 10.1177/0892705719833105.

[2] A. K. Sinha, H. K. Narang, and S. Bhattacharya, "Mechanical properties of natural fiber polymer composites," *Journal of Polymer Engineering*, vol. 37, no. 9, pp. 879–895, 2017, doi: 10.1515/polyeng-2016-0362.

[3] Diaz, L. J. Leslie, S. M. Hagad, and P. J. M. Santiago, "Minimizing property variation in natural fiber reinforcements for green composite materials applications," *Materials Science Forum*, vol. 894, pp. 50–55, 2017, doi: 10.4028/www.scientific.net/MSF.894.50.

[4] R. Biswas, N. Sharma, and K. K. Singh, "Numerical analysis of mechanical and fatigue behaviour of glass and carbon fiber reinforced polymer composite," *Materials Today: Proceedings*, 2023, doi: 10.1016/j.matpr.2023.03.479.

[5] I. Suyambulingam, S. M. Rangappa, and S. Siengchin, "Advanced materials and technologies for engineering applications," *Applied Science and Engineering Progress*, vol. 16, no. 3, 2023, Art. no. 6760, doi: 10.14416/j.asep.2023.01.008.

[6] S. K. Palaniappan, M. K. Singh, S. M. Rangappa, and S. Siengchin, "Eco-friendly biocomposites: A step towards achieving sustainable development goals," *Applied Science and Engineering Progress*, vol. 17, no. 4, Art. no. 7373, 2024, doi: 10.14416/j.asep.2024.02.003.

[7] B. Ma'ruf, A. Ismail, D. P. Sari, and S. H. Sujiatanti, "Strength analysis of marine biaxial warp-knitted glass fabrics as composite laminations for ship material," *Curved and Layered Structures*, vol. 10, 2023, doi: 10.1515/cls-2022-0209.

[8] S. B. Koppula, S. Karachi, V. Kumar, N. D. Borra, Y. Phaneendra, V. S. Neigapula, and S. Hemalatha, "Investigation into the mechanical characteristics of natural fiber-reinforced polymer composites: Effects of flax and e-glass reinforcement and stacking configuration," *Materials Today: Proceedings*, 2023, doi: 10.1016/j.matpr.2023.07.020.

[9] B. Parveez, M. I. Kittur, I. A. Badruddin, S. Kamangar, M. Hussien, and M. A. Umarfarooq, "Scientific advancements in composite materials for aircraft applications: A review," *Polymers*, vol. 14, no. 22, 2022, doi: 10.3390/polym14225007.

[10] M. Ramesh, K. Palanikumar, and K. H. Reddy, "Mechanical property evaluation of sisal-jute-glass fiber reinforced polyester composites," *Composites Part B: Engineering*, vol. 48, pp. 1–9, 2013, doi: 10.1016/j.compositesb.2012.12.004.

[11] G. B. V. Kumar, R. Mageshvar, R. Rejath, S. Karthik, R. Pramod, and C. S. P. Rao, "Characterization of glass fiber bituminous coal tar reinforced polymer matrix composites for high performance applications," *Composites Part B: Engineering*, vol. 175, 2019, Art. no. 107156, doi: 10.1016/j.compositesb.2019.107156.

[12] S. Klara, F. Mahmuddin, and M. Muas, "Analysis of loading change effect to boat velocity on a 2.5 GT fishing FRP boat with a field

test," *SPECTA Journal of Technology*, vol. 2, no. 1, pp. 5–10, 2018, doi: 10.35718/specta.v2i1.89.

[13] I. Yusuf, A. Yani, and M. S. Baba, "Approaches method to solve ships routing problem with an application to the Indonesian national shipping company," in *Proceedings of the 2011 International Conference on Applied, Numerical and Computational Mathematics*, pp. 57–62, 2011, doi: 10.5555/2047950.2047959.

[14] S. Jayaram, K. Sivaprasad, and C. G. Nandakumar, "Recycling of FRP Boats," *International Journal of Advanced Research in Engineering and Technology*, vol. 9, no. 3, pp. 244–252, 2018.

[15] N. Kumar, S. Kumar, J. S. Grewal, V. Mehta, and S. Ali, "Comparative study of Abaca fiber and Kevlar fibers based brake friction composites," *Polymer Composites*, vol. 43, no. 2, pp. 730–740, 2022, doi: 10.1002/pc.26405.

[16] T. Fulga and M. Zanoaga, "Fiber reinforced polymer composites as structuaral materials for aeronauctics," in *International Conference of Scientific Paper AFASES*, pp. 1–10, 2013.

[17] P. D. Mangalgiri, "Composite materials for aerospace applications," *Bulletin of Materials Science*, vol. 22, pp. 657–664, 1999, doi: 10.1007/BF02749982.

[18] R. Pramod and S. Kumar, "Evaluation of mechanical and insulation properties of nomex-t410 and H.S. glass polymer matrix composites," *Materials Today: Proceedings*, vol. 4, no. 2, pp. 3233–3242, 2017, doi: 10.1016/j.matpr.2017.02.209.

[19] O. Demircan, C. Yilmaz, E. S. Kocaman, and M. Yildiz, "An experimental study on tensile and bending properties of biaxial warp knitted textile composites," *Advanced Composite Materials*, vol. 29, pp. 73–88, 2020, doi: 10.1080/09243046.2019.1639016.

[20] R. Pramod, S. Basavarajappa, G. B. V. Kumar, and M. Chavali, "Drilling induced delamination assessment of nanoparticles reinforced polymer matrix composites," *Journal of Mechanical Engineering Science*, vol. 236, pp. 2931–2948, 2022, doi: 10.1177/09544062211030967.

[21] K. K. Singh, M. T. Ansari, and M. S. Azam, "Fatigue life and damage evolution in woven GFRP angle ply laminates," *International Journal of Fatigue*, vol. 142, 2021, Art. no. 105964, doi: 10.1016/j.ijfatigue.2020.105964.

[22] S. A. Khan, S. S. R. Koloor, K. J. Wong, T. Dickhut, and M. N. Tamin, "An interlaminar fatigue damage model based on property degradation of carbon fiber-reinforced polymer composites," *Engineering Fracture Mechanics*, vol. 302, 2024, Art. no. 110066, doi: 10.1016/j.engfracmech.2024.110066.

[23] O. Y. Burak, L. Parnas, and D. Coker, "Interlaminar tensile strength of different angle-ply CFRP composites," *Procedia Structural Integrity*, vol. 21, pp. 198–205, 2019, doi: 10.1016/j.prostr.2019.12.102.

[24] K. A. Eldressi, H. M Alojaly, W. O. A. Salem, and Naser S. Sanoussi, "Review of recent developments in polymer matrix composites with particulate reinforcements," *Comprehensive Materials Processing*, pp. 409–413, 2024, doi: 10.1016/B978-0-323-96020-5.00067-4.

[25] G. Chen, A. Li, H. Liu, S. Huang, Z. Zhang, W. Liu, C. Zha, B. Li, and Z. Wang, "Mechanical and dynamic properties of resin blend and composite systems: A molecular dynamics study," *Composite Structures*, vol. 190, pp. 160–168, 2018, doi: 10.1016/j.compstruct.2018.02.001.

[26] Y. Lyu and H. Ishida, "Natural-sourced benzoxazine resins, homopolymers, blends and composites: A review of their synthesis, manufacturing and applications," *Progress in Polymer Science*, vol. 99, 2019, Art. no. 101168, doi: 10.1016/j.progpolymsci.2019.101168.

[27] F. C. Fernandes, K. Kirwan, D. Lehane, and S. R. Coles, "Epoxy resin blends and composites from waste vegetable oil," *European Polymer Journal*, vol. 89, pp. 449–460, 2017, doi: 10.1016/j.eurpolymj.2017.02.005.

[28] M. M. Raj, L. M. Raj, and P. N. Dave, "Glass fiber reinforced composites of phenolic–urea–epoxy resin blends," *Journal of Saudi Chemical Society*, vol. 16, no. 3, 2012, doi: 10.1016/j.jscs.2011.01.007.

[29] A. Toldy, Á. Szlancsik and B. Szolnoki, "Reactive flame retardancy of cyanate ester/epoxy resin blends and their carbon fibre reinforced composites," *Polymer Degradation and Stability*, vol. 128, pp. 29–38, 2016, doi: 10.1016/j.polymdegradstab.2016.02.015.

[30] A. A. Athawale and J. A. Pandit, "Chapter 1 - Unsaturated polyester resins, blends, interpenetrating polymer networks, composites, and nanocomposites: State of the art and new challenges," in *Unsaturated Polyester Resins*. Amsterdam, Netherlands: Elsevier, pp. 1–42, 2019, doi: 10.1016/B978-0-12-816129-6.00001-6.

[31] H. N. Dhakal and S. O. Ismail, "Chapter 8 - Unsaturated polyester resins: Blends, interpenetrating polymer networks, composites, and nanocomposites,"

in *Unsaturated Polyester Resins*. Amsterdam, Netherlands: Elsevier, 2019, pp. 181–198, 2019, doi: 10.1016/B978-0-12-816129-6.00008-9.

[32] B. K. Kandola, L. Krishnan, and J. R. Ebdon, "Blends of unsaturated polyester and phenolic resins for application as fire-resistant matrices in fibre-reinforced composites: Effects of added flame retardants," *Polymer Degradation and Stability*, vol. 106, pp. 129–137, 2014, doi: 10.1016/j.polymdegradstab.2013.12.021.

[33] C. Liu, H. Yuhong, M. Sun, X. Zhang, B. Zhang, and X. Bai, "Influence of epoxy resin species on the curing behavior and adhesive properties of cyanate Ester/Poly(aryl ether nitrile) blends," *Polymer*, vol. 288, 2023, Art. no. 126450, doi: 10.1016/j.polymer.2023.126450.

[34] X. Guo, K. Wei, N. Tengfei, W. Shi, C. Dai, Z. Zhao, and G. Zhanpeng, "Preparation and performance analysis of polyethylene glycol/ epoxy resin composite phase change material," *Journal of Energy Storage*, vol. 88, 2024, Art. no. 111525, doi: 10.1016/j.est.2024.111525.

[35] G. B. V. Kumar, R. Mageshvar, R. Rejath, S. Karthik, R. Pramod, and C. S. P. Rao, "Characterization of glass fiber bituminous coal tar reinforced Polymer Matrix Composites for high performance applications *Composites Part B: Engineering*, vol. 175, 2019, Art. no. 107156, doi: 10.1016/j.compositesb.2019.107156.

[36] J. J. Lu, Y. C. Shi, J. P. Guan, R. Q. Dang, L. C. Yu, H. Q. Wang, N. D. Hu, and X. J. Shen, "Enhanced mechanical properties of ramie fabric/epoxy composite laminates by silicon polymer," *Industrial Crops and Products*, vol. 199, 2023, Art. no. 116778, doi: 10.1016/ j.indcrop.2023.116778.

[37] M. S. Sarfraz, H. Hong, and S. S. Kim, "Recent developments in the manufacturing technologies of composite components and their cost-effectiveness in the automotive industry: A review study," *Composite Structures*, vol. 266, 2021, Art. no. 113864, doi: 10.1016/j.compstruct. 2021.113864.

[38] G. Chollon, O. Siron, J. Takahashi, H. Yamauchi, K. Maeda, and K. Kosaka, "Microstructure and mechanical properties of coal tar pitch-based 2D-C/C composites with a filler addition," *Carbon*, vol. 39, pp. 2065–2075, 2001, doi: 10.1016/ S0008-6223(01)00021-5.

[39] S. Sembiring, A. Riyanto, R. Situmeang, and Z. Sembiring, "Bituminous composite comprising amorphous Silica from rice husks," *Ceram – Silikaty*, vol. 63, pp. 277–286, 2019, doi: 10.13168/cs.2019.0021.

[40] V. Mahesh, S. Joladarashi, and S. M. Kulkarni, "A comprehensive review on material selection for polymer matrix composites subjected to impact load," *Defence Technology*, vol. 17, no. 1, pp. 257–277, 2021, doi: 10.1016/j.dt.2020.04.002.

[41] R. Laghaei, S. M. Hejazi, H. Fashandi, S. Akbarzadeh, S. Shaghaghi, and A. S. Kashani, "Improvement in fracture toughness and impact resistance of E-glass/epoxy composites using layers composed of hollow poly(ethylene terephthalate) fibers," *Journal of Industrial Textiles*, vol. 51, no. 3, 2022, doi: 10.1177/15280837211044910.

[42] T. P. Mohan and K. Kanny, "Dynamic mechanical analysis of glass fiber reinforced Epoxy filled nanoclay hybrid composites," *Materials Today: Proceedings*, vol. 87, no. 1, pp. 235–245, 2023, doi: 10.1016/j.matpr.2023.05.282.

[43] K. Arunprasath, M. Vijayakumar, M. Ramarao, T. G. Arul, S. P. Pauldoss, M. Selwin, B. Radhakrishnan, and V. Manikandan, "Dynamic mechanical analysis performance of pure 3D printed polylactic acid (PLA) and acrylonitrile butadiene styrene (ABS)," *Materials Today: Proceedings*, vol. 50, no. 5, pp. 1559–1562, 2022, doi: 10.1016/j.matpr.2021.09.113.

[44] Z. Weng, J. Wang, T. Senthil, and L. Wu, "Mechanical and thermal properties of ABS/montmorillonite nanocomposites for fused deposition modeling 3D printing," *Materials & Design*, vol. 102, pp. 276–283, 2016, doi: 10.1016/j.matdes.2016.04.045.

[45] Mishra, Kunal, L. K. Babu, D. Dhakal, P. Lamichhane, and R. K. Vaidyanathan, "The effect of solvent on the mechanical properties of polyhedral oligomeric silsesquioxane (POSS)–epoxy nanocomposites," *SN Applied Sciences*, vol. 1, pp. 1–7, 2019, Art. no. 898, doi: 10.1007/ s42452-019-0918-1.

[46] K. Arunprasath, M. Vijayakumar, M. Ramarao, T.G. Arul, S. P. Pauldoss, M. Selwin, B. Radhakrishnan, and V. Manikandan, "Dynamic mechanical analysis performance of pure 3D printed polylactic acid (PLA) and acrylonitrile butadiene styrene (ABS)," *Materials Today: Proceedings*, vol. 50, no. 5, pp. 1559–1562, 2022, doi: 10.1016/j.matpr.2021.09.113.

[47] J. Feng and Z. Guo, "Temperature-frequency-dependent mechanical properties model of epoxy resin and its composites," *Composites*

Part B: Engineering, vol. 85, pp. 161–169, 2016, doi: 10.1016/j.compositesb.2015.09.040.

[48] C. Li, R. Zhang, G. Wang, and Y. Shi, "The mechanical properties of epoxy resin composites modified by compound modification," *AIP Advances*, vol. 8, no. 10, 2018, Art. no. 105325, doi: 10.1063/1.5047083.

[49] J. Tang, H. Zhou, Y. Liang, X. Shi, X. Yang, and J. Zhang, "Properties of graphene oxide/epoxy resin composites," *Journal of Nanomaterials*, vol. 2014, 2014, Art. no. 696859, doi: 10.1155/2014/696859.

[50] T. V. Brantseva, Y. A. Gorbatkina, V. Dutschk, K. Schneider, and R. Häßler, "Modification of epoxy resin by polysulfone to improve the interfacial and mechanical properties in glass fibre composites. III. Properties of the cured blends and their structures in the polymer/fibre interphase," *Journal of Adhesion Science and Technology*, vol. 18, pp. 1309–1323, 2004, doi: 10.1163/1568561041588183.

[51] L. Tao and Zey, "Improving the toughness of thermosetting epoxy resins via blending triblock copolymers," *RSC Advances*, vol. 10, pp. 1603–1612, 2020, doi: 10.1039/c9ra09183a.

[52] J. N. Martins, T. G. Klohn, O. Bianchi, R. Fiorio, and E. Freire, "Dynamic mechanical, thermal, and morphological study of ABS/textile fiber composites," *Polymer bulletin*, vol. 64, pp. 497–510, 2010, doi: 10.1007/s00289-009-0200-6.

[53] X. F. Liu, X. Luo, B. W. Liu, H. Y. Zhong, D. M. Guo, R. Yang, L. Chen, and Y. Z. Wang, "Toughening epoxy resin using a liquid crystalline elastomer for versatile application," *ACS Applied Polymer Materials*, vol. 1, no. 9, pp. 2291–2301, 2019, doi: 10.1021/acsapm.9b00319.

[54] G. Youssef, S. Newacheck, N. U. Huynh and C. Gamez, "Multiscale characterization of e-glass/epoxy composite exposed to extreme environmental conditions," *Journal of Composites Science*, vol. 5, no. 3, 2021, doi: 10.3390/jcs5030080.

[55] N. Gökçe, S. Eren, M. Nodehi, D. Ramazanoğlu, S. Subaşi, O. Gencel, and T. Ozbakkaloglu, "Engineering properties of hybrid polymer composites produced with different unsaturated polyesters and hybrid Epoxy," *Journal of Building Engineering*, vol. 89, 2024, Art no. 109334, doi: 10.1016/j.jobe.2024.109334.

[56] Sun, Zeyu, L. Xu, Z. Chen, Y. Wang, R. Tusiime, C. Cheng, S. Zhou, Y. Liu, M. Yu, and H. Zhang, "Enhancing the mechanical and thermal properties of epoxy resin via blending with Thermoplastic Polysulfone," *Polymers*, vol. 11, no. 3, 2019, doi: 10.3390/polym11030461.

[57] H. Xu, X. Zhang, Y. Yating, Y. Yang, and L. Weng, "Enhanced adhesion property of epoxy resin composites through dual reinforcement mechanisms," *Next Materials*, vol. 3, 2024, Art. no. 100072, doi: 10.1016/j.nxmate.2023.100072.

[58] K. Devendra and T. Rangaswamy, "Strength characterization of e-glass fiber reinforced epoxy composites with filler materials," *Journal of Minerals and Materials Characterization and Engineering*, vol. 1, no. 6, pp. 353–357, 2013, doi: 10.4236/jmmce.2013.16054.

[59] Y. Zeng, Y. Xue, X. Gong, X. Gao, E. Jiaqiang, J. Chen, and E. Leng, "Pyrolytic performance and kinetics study of epoxy resin in carbon fiber reinforced composites: Synergistic effects of epoxy resin and carbon fiber," *Journal of Analytical and Applied Pyrolysis*, vol. 176, 2023, Art. no. 106255, doi: 10.1016/j.jaap.2023.106255.

[60] Z. Tuo, K. Chen, Q. Zhou, Y. Wang, Q. Wang, Y. Zhang, Z. Lin, and Y. Liang, "High-performance shape memory epoxy resin with high strength and toughness: Prepared by introducing hydrogen bonds through polycaprolactone and low melting point alloy," *Composites Science and Technology*, vol. 250, 2024, Art. no. 110510, doi: 10.1016/j.compscitech.2024.110510.

[61] M. Gopalakrishnan, S. Muthu, R. Subramanian, R. Santhanakrishnan, and L. M. Karthigeyan, "Tensile properties study of E-glass/epoxy laminate and π/4 quasi-isotropic E-glass/epoxy laminate," *Polymers and Polymer Composites*, vol. 24, pp. 429–446, 2016, doi: 10.1177/096739111602400606.

[62] D. Hwang and D. Cho, "Fiber aspect ratio effect on mechanical and thermal properties of carbon fiber/ABS composites via extrusion and long fiber thermoplastic processes," *Journal of Industrial and Engineering Chemistry*, vol. 80, pp. 335–344, 2019, doi: 10.1016/j.jiec.2019.08.012.

[63] M. M. Singh, H. Kumar, G. H. Kumar, P. Sivaiah, K. V. Nagesha, K. M. Ajay, and G. Vijaya "Determination of strength parameters of glass fibers reinforced composites for engineering applications," *Silicon*, vol. 12, pp. 1–11, 2020, doi: 10.1007/s12633-019-0078-3.

[64] Y. Qi, Q. Fan, J. Li, Q. Cao, X. Pan, Y. Pan, X. Jian, and Z. Weng, "Toughened and reinforced the petroleum-based epoxy resin via thermotropic liquid crystal bio-based counterpart," *Composites Communications*, vol. 44, 2023, Art. no. 101771, doi: 10.1016/j.coco.2023.101771.

[65] C. B. Luna, E. B. Ferreira, D. D. Siqueira, E. A. Filho, and E. M. Araújo, "Additivation of the ethylene–vinyl acetate copolymer (EVA) with maleic anhydride (M.A.) and dicumyl peroxide (DCP): the impact of styrene monomer on crosslinking and functionalization," *Polymer Bulletin*, vol. 79, pp. 7323–7346, 2021, doi: 10.1007/s00289-021-03856-x.